Characterization of Protein−DNA Interactions Using Surface Plasmon Resonance Spectroscopy with Various Assay Schemes

Huey Fang Teh,[‡] Wendy Y. X. Peh,[‡] Xiaodi Su,*[,‡] and Jane S. Thomsen*[,§]

Institute of Materials Research and Engineering, 3 Research Link, Singapore 117602, and Genome Institute of Singapore, 60 Biopolis Street, Singapore 117528

Received September 13, 2006; Revised Manuscript Received November 1, 2006

ABSTRACT: Specific protein−DNA interactions play a central role in transcription and other biological processes. A comprehensive characterization of protein−DNA interactions should include information about binding affinity, kinetics, sequence specificity, and binding stoichiometry. In this study, we have used surface plasmon resonance spectroscopy (SPR) to study the interactions between human estrogen receptors (ER, α and *β* subtypes) and estrogen response elements (ERE), with four assay schemes. First, we determined the sequence-dependent receptors' binding capacity by monitoring the binding of ER to various ERE sequences immobilized on a sensor surface (assay format denoted as the direct assay). Second, we screened the relative affinity of ER for various ERE sequences using a competition assay, in which the receptors bind to an ERE-immobilized surface in the presence of competitor ERE sequences. Third, we monitored the assembly of ER−ERE complexes on a SPR surface and thereafter the removal and/or dissociation of the ER (assay scheme denoted as the dissociation assay) to determine the binding stoichiometry. Last, a sandwich assay (ER binding to ERE followed by anti-ER recognition of a specific ER subtype) was performed in an effort to understand how ERα and ER*β* may associate and compete when binding to the DNA. With these assay schemes, we reaffirmed that (1) ERα is more sensitive than ER*β* to base pair change(s) in the consensus ERE, (2) ERα and ER*β* form a heterodimer when they bind to the consensus ERE, and (3) the binding stoichiometry of both ERα− and ER*β*−ERE complexes is dependent on salt concentration. With this study, we demonstrate the versatility of the SPR analysis. With the involvement of various assay arrangements, the SPR analysis can be further extended to more than kinetics and affinity study.

Sequence specific protein−DNA binding events play many key roles in cells, including the dominant roles in the regulation of gene expression. To characterize protein−DNA interactions, people have largely relied on conventional biochemistry methods, including DNase I footprinting assays, gel mobility shift assays, filter binding assays, and genetic analysis. With these methods, one can quantify the binding affinity, measure the on- and off-rates, localize binding sites, and study sequence specificity. Most of these methods, however, use biohazard labels and involve tedious assay steps that need extensive optimizations (*1*).

The surface plasmon resonance (SPR) technique, a label-independent technique, has emerged as a powerful alternative to conventional biochemistry methods for studying bioaffinity interactions (*2*−*5*), including protein−DNA binding that may involve purified proteins (*6*−*14*) and a multiprotein complex in nuclear extracts (*11*, *15*). Most of these studies, however, use a basic assay design to monitor the binding of protein to surface-immobilized DNA or the binding of DNA to immobilized protein (*14*) with the aims of determining the binding kinetics (*10*), thermodynamics (*6*, *10*, *12*), or sequence-dependent binding amount (*12*−*15*).

In our recent study of protein−DNA binding, particularly estrogen receptors (ER, α and *β* subtypes) binding to their consensus response elements (ERE), we found that the potential of the SPR analysis can be further extended with the use of versatile assay arrangements derived from traditional biochemistry methods.

In gel mobility assays, for example, protein and a radiolabeled restriction DNA fragment containing one or more binding sites for the protein studied are first incubated in solution. When the complex forms, samples are applied onto a polyacrylamide gel for electrophoretic separation of the protein-bound DNA and unbound DNA. The migration profile and the intensity of the radioactive protein−DNA bands indicate the presence of the protein−DNA complex (*1*). To investigate the sequence specificity of the binding, competition experiments are often carried out. A competitor DNA (normally a synthetic oligonucleotide) is added to the protein and DNA mixture to compete for the binding site of the protein (*16*). If the competitor affects the intensity of the protein−DNA complex band, the sequence of the competitor is known to have a strong affinity for the protein. In gel mobility assays, when one uses a protein mixture, it is not clear which protein is binding to the DNA; thus, an antibody against the particular protein of interest can be

* To whom correspondence should be addressed. X.S.: telephone, 65-68748420; fax, 65-68720785; e-mail, xd-su@imre.a-star.edu.sg. J.S.T.: telephone, 65-64788179; fax, 65-64789060; e-mail, thomsenj@gis.a-star.edu.sg.

[‡] Institute of Materials Research and Engineering.

[§] Genome Institute of Singapore.

10.1021/bi061903t CCC: $37.00
Published on Web 02/01/2007

Table 1: Sequences of EREs Involved in This Study

name	sequence
GREB1	5′-biotin-TGTGGCAACTGGGTCATTCTGACCTAGAAGCAAC-3′
vitellogenin	5′-biotin-GTCCAAAGTCAGGTCACAGTGACCTGATCAAAGT-3′
mutant-vitellogenin	5′-biotin-GTCCAAAGTCAG***T***TCACAGTGA***T***CTGATCAAAGT-3′
pS2	5′-biotin-TCCCCCTGCAAGGTCACGGTG***G***CCACCCCGTGAG-3′
mutant-pS2	5′-biotin-TCCCCCTGCAAGGT***T***ACGGTGGTCACCCC***GT***GAG-3′
scrambled	5′-biotin-GTCCAAAGTCAATCGCCAGCACGATGATCAAAGT-3′

added in a secondary incubation step to supershift the complex bands to determine if the protein of interest is bound to the DNA (*17*). These refinements to the basic methodology provide additional types of information.

In this study, we introduce similar modifications to the basic SPR approach, denoted as the direct assay [name borrowed from immunoassay approaches (*18*)], with the aim of achieving a comprehensive characterization of ERs and ERE interactions in various aspects. Besides the direct assay scheme, with which we compare the sequence-dependent ERα and ERβ binding amount, we transfer the competition assay approach onto the SPR platform and monitor the receptor's binding with the presence of competitor sequences. With this approach, we screen the relative affinity of the receptors for several ERE sequences (e.g., chicken vitellogenin A2, human pS2, human GREB1, and their mutant sequences), with immobilization of only one sequence on the SPR surface. We also adopt a sandwich assay, i.e., using anti-ERα in a successive step, to identify bound ERα from a receptor mixture and hence to determine how ERα and ERβ may associate and/or compete to bind to ERE. Last, we develop a new assay scheme (denoted as the dissociation assay) to monitor the assembly of protein−DNA complexes formed in solution (as in the gel mobility assay) on the SPR surface and thereafter the dissociation of the protein from the surface. With this approach, we determine ER−ERE binding stoichiometry.

ERα and ERβ are members of the nuclear receptor superfamily of transcription factors. Binding of ER to DNA of specific sequences known as estrogen response elements (EREs) is a critical step in gene regulation. Among various natural EREs, ERα and ERβ are known to bind with highest affinity to the perfect ERE sequence of two 5 bp half-sites, GGTCA, organized as inverted repeats with a 3 bp spacing (*16*, *17*). Imperfect ERE sequences differing by one or more nucleotides are known to decrease the binding affinity (*12*).

In addition to the sequence-dependent binding affinity, other characteristics like ER−ERE binding stoichiometry, and how ERα and ERβ may compete or associate when they bind to ERE are all important issues underlying their gene regulation mechanism. The comprehensive SPR characterization of these issues, using different assay schemes, complements the studies using conventional gel mobility assays (*10*, *16*, *17*, *19*−*21*) and the studies using a SPR technique with only the direct assay scheme (*10*−*12*, *22*).

MATERIALS AND METHODS

Materials. Partially purified recombinant human ERα and ERβ (>80% pure) were purchased from PanVera Corp. (Madison, WI). They were stocked in HEPES buffer containing 10% glycerol. For long-term storage, the ER proteins were stored in aliquots of 10 μL at −80 °C. Before use, the aliquots were thawed in a room-temperature water bath and were diluted using HEPES buffer [40 mM HEPES-KOH binding buffer (pH 7.4) containing 10 mM $MgCl_2$, 0.2% Triton X-100, and 2 mM DTT], containing either 100 or 200 mM KCl, to form solutions with desired concentrations. Rabbit anti-human ERα polyclonal antibody (HC-20) was purchased from Santa Cruz Biotechnology (Santa Cruz, CA).

Six 34 bp, HPLC-purified ERE-containing oligos (synthesized by PROLIGO Primers & Probes, Boulder, CO) were used in this study. The sequences of the biotinylated strands of these oligos are listed in Table 1. The chicken vitellogenin A2 ERE (*23*) (denoted as vit ERE) and human GREB1 (*24*) ERE both contain a perfect ERE core sequence, GGTCAnnnTGACC, but have different flanking and spacing sequences. The human pS2 ERE (*25*) has a core sequence that differs from the consensus core by 1 bp (bold) in the 3′ half-site. Both the vit and pS2 EREs are mutated to form mt-vit and mt-pS2 EREs, respectively, by introduction of symmetric base substitutions (bold) in each of their ERE half-sites. A sequence-scrambled DNA (denoted as scr DNA) that contains non-ERE sites was used as a negative control. The biotinylated strands and the antistrands were annealed in phosphate-buffered saline (PBS, pH 7.4) containing 10 mM EDTA (pH 7.5) and stored at −27 °C.

A PBS buffer [10 mM phosphate buffer (pH 7.4) and 150 mM NaCl] was used as a carrier buffer for streptavidin (SA) (Sigma-Aldrich) and DNA assembly and the HEPES buffer for ER−ERE interactions and anti-ERα binding.

SPR Apparatus and Gold Disk Surface Preparation. The SPR measurements were conducted using an AutoLab ESPR instrument (Eco Chemie), a double-channel and prism coupling-based instrument. A gold-coated glass disk mounted on a prism through a thin layer of index-matching oil forms the base of a two-channel cuvette. Different samples can be added into the two independent channels. In the kinetic measurement mode, molecular binding on gold-coated glass disks is followed by monitoring the SPR angle (θ) over time. The measured angle shifts ($\Delta\theta$) correspond to the amount of adsorbed material with a mass sensitivity factor of 120 mdeg per 100 ng/cm^2 (*26*). The measurements were conducted at room temperature, and the noise level in $\Delta\theta$ measurement was 0.5 mdeg.

Streptavidin-modified surfaces were used throughout the study. For SA immobilization, freshly cleaned gold disks (10 min under UV and ozone followed by 2 min with hot piranha solution, Caution!) were treated overnight with a binary biotin-containing thiol mixture of 10% biotin-PEG disulfide (LCC Engineering & Trading GmbH) and 90% 11-mercapto-1-undecanol (Sigma, St. Louis, MO) at a net concentration of 1 mM in ethanol (*27*). After the samples were rinsed with ethanol which was followed by a drying

Scheme 1: Assay Schemes Used in This Study

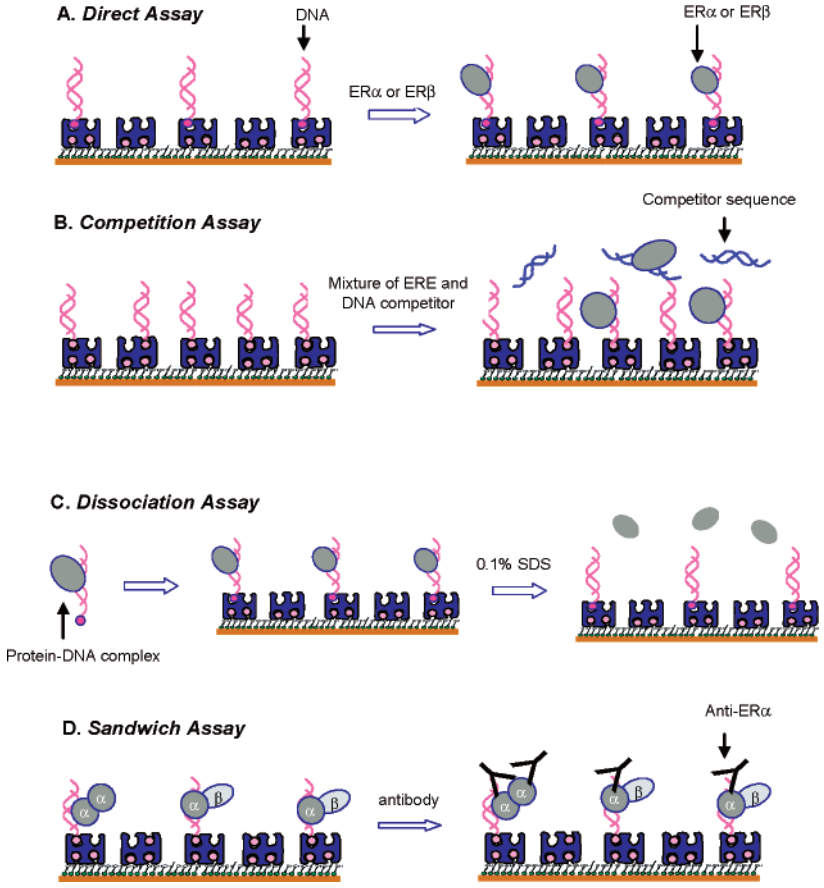

step using nitrogen, SA (0.1 mg/mL) was added to bind to the surface through one or two of its biotin binding sites while others remain exposed. On the Autolab ESPR equipment, a perfect preparation of a SA film leads to a SPR angle shift of ~440 mdeg (*26*). The subsequent DNA assembly amount is concentration-dependent (see the Supporting Information). This biotin- and thiol-based surface chemistry has been proven to be highly reliable, ensuring a reproducible streptavidin immobilization and DNA assembly (relative standard deviation of ~5%) (*26*).

Assay Procedures. Scheme 1 shows the assay schemes used in this study. In the direct assay, competition assay, and sandwich assay, ERE sequences were immobilized on the SA surface from solutions of 500 nM (for the direct assay and competition assay) or 20 nM (for the sandwich assay), which leads to either maximal DNA binding or diluted DNA binding, respectively (see the Supporting Information). In the direct assay, the receptors (ER) were applied to react with the immobilized DNA for 30 min. The assay procedure of the competition assay is similar to that of the direct assay, except that the receptors at a fixed concentration of 110 nM were preincubated with 1-, 3-, 5-, 8-, 10-, or 20-fold excesses of competitor EREs (non-biotinylated) for 30 min at room temperature, prior to application to an ERE-immobilized surface. In the sandwich assay, receptor binding (from a mixture of ERα and ERβ) is followed by anti-ERα (10 μg/mL) recognition of bound ERα. In this experiment, the use of diluted DNA (from a 20 nM solution) ensures sufficient space between DNA strands for receptors and antibody to bind. In the dissociation assay, 50 nM ERα or ERβ was preincubated with 500 nM biotinylated ERE for 30 min in HEPES buffer at room temperature, prior to application to the SA-modified surface. The assembly of the ER−ERE complex was monitored, followed by the removal (dissociation) of the bound receptors with 0.1% sodium dodecyl sulfate (SDS).

To regenerate the immobilized DNA surface or dissociate the ER−ERE complex (as mentioned above), SDS was added to the liquid cell and the sample incubated for 2−3 min. HEPES buffer was then applied to replace the SDS and to reset the baseline for new cycles of receptor binding.

RESULTS AND DISCUSSION

Direct Assay for Studying Sequence Specificity. In the direct assay approach (Scheme 1A), the tested ERE sequences are immobilized from DNA solutions at a fixed concentration (500 nM) to ensure identical DNA surface density. Figure 1 is a SPR sensorgram showing the immobilization of SA, followed by the assembly of biotinylated pS2 ERE and its mutant form (mt-pS2) in different SPR channels. After the baseline has been set in HEPES buffer, ER solutions are applied. Control experiments conducted by introducing ER solutions on a SA-modified surface with no immobilized ERE (the inset of Figure 1) show only a reversible buffer effect but no nonspecific ERα and ERβ adsorption. Thus, the SPR angle shifts ($\Delta\theta$) recorded in HEPES buffer before and after ER binding are specific to binding of the receptor to DNA. After each cycle of receptor binding, a short treatment of the surface using 0.1% SDS, together with a rinsing step with HEPES buffer, dissociates the ER−DNA complexes and exposes the immobilized EREs

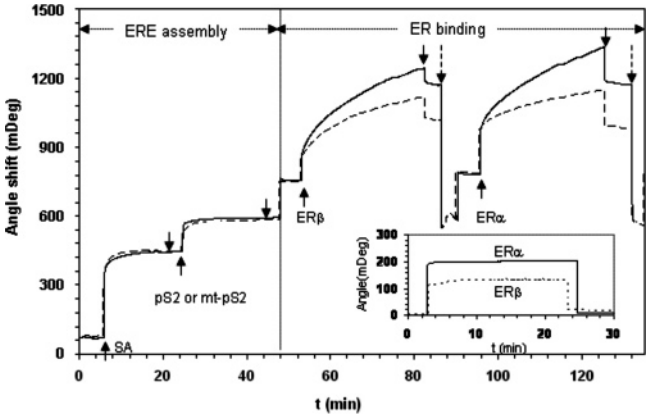

FIGURE 1: SPR sensorgrams showing the ERE assembly on a SA-treated surface and binding of ERβ and ERα to the immobilized ERE. Two ERE sequences, pS2 (—) and mt-pS2 (- - -), were assembled in two different channels from a 500 nM PBS solution. Binding of the receptors was from a 110 nM HEPES solution. The down arrows indicate the time when the surface is rinsed with the representative buffers. The dashed arrows indicate the time when 0.1% SDS is applied to dissociate the bound protein. The application of a receptor solution leads to a rapid SPR angle shift ($\Delta\theta$) in the first few seconds, followed by a much slower increase. The initial rapid angle shift is mainly due to the change in the bulk refractive index, as the protein solution contains some glycerol (see Materials and Methods) absent in the background HEPES buffer. At the end of protein binding, rinsing with HEPES buffer corrects the bulk buffer effect and washes away loosely attached ER protein (if there is any). The inset shows the ERα (—) and ERβ (- - -) application on a SA-treated surface with no ERE immobilization. We observed only a reversible buffer effect but no nonspecific protein binding.

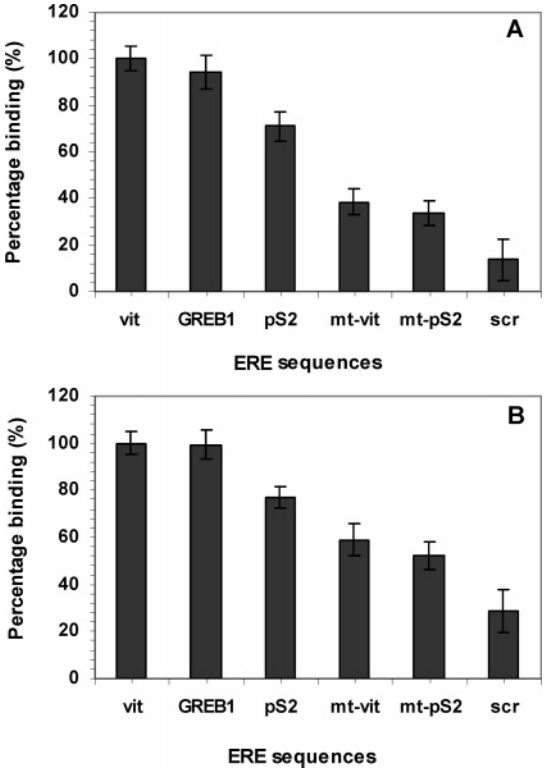

FIGURE 2: Sequence-dependent binding (%) of ERα (A) and ERβ (B) to various ERE sequences determined using the direct assay. The receptor concentration that was used was 110 nM for both ERα and ERβ. Binding buffer is HEPES containing 100 mM KCl. Each individual ERE sequence is immobilized on a SPR surface with identical surface coverage ($\Delta\theta = 135.1 \pm 4.1$; RSD $\sim$ 3%), to ensure the measured receptor bindings are determined by sequence variations. The error bar is derived from three duplication experiments.

substantially, as evidenced by the retainable baseline. This regeneration strategy is applied to all of the following assay schemes.

In Figure 1, the surface densities of the immobilized pS2 and mt-pS2 EREs are identical [$\Delta\theta = 128.4 \pm 2.2$ mdeg; relative standard deviation (RSD) of <2%]. In the successive steps of receptor binding, the SPR responses in the two channels are significantly different, with those in the pS2 channel being consistently higher than in the mt-pS2 channel, for both ERα and ERβ.

A whole series of direct assay experiments were similarly carried out, involving the other EREs (Table 1). Each individual sequence was immobilized in separate experiments for ERα and ERβ to bind. Figure 2 summarizes the receptor binding signals (normalized to the amount of ER binding to the vit ERE) at a fixed receptor concentration of 110 nM. The surface density of the immobilized EREs in these experiments is identical (RSD $\sim$ 3%), ensuring that the measured receptor binding signals are dependent on ERE sequences. For both of the two ER subtypes, we observed the following order of binding signals: vit $\cong$ GREB1 > pS2 > mt-vit $\geq$ mt-pS2 > scr DNA. As expected, the consensus EREs (chicken vit and human GREB1) exhibit similar affinity, being the highest among the tested sequences, due to the presence of the perfect core sequence (GGTCAnnnTGACC). Different flanking sequences and spacing sequences in these EREs lead to no obvious difference in receptor binding ability in our system. In the pS2 ERE, one base pair change in the 3′ half-site of the ERE core sequence causes hydrogen bond substitutions and also a rearrangement of a localized hydrogen bond network in the receptor−DNA complexes (*16*), therefore weakening the receptor binding, which is evidenced by the reduced receptor binding signals. When the ERE core sequences are further mutated to contain more base pair changes (mt-vit and mt-pS2), the contacts between the protein and the DNA are further disrupted, as shown by the even weaker binding signals. The observed receptor binding signals reflect these trends well. Interestingly, we found that both ERα and ERβ exhibit detectable nonspecific binding with the sequences of scrambled DNA, the β subtype to a greater extent.

Comparison of sequence-dependent receptor binding signals within Figure 2A (for ERα) and Figure 2B (for ERβ) shows that ERα is more sensitive to sequence variation than ERβ. For the mt-vit and mt-pS2 sequences, for example, the level of ERα binding dropped ~60%, whereas the level of ERβ binding dropped ~40%. This result obtained with the involvement of more ERE sequences concurs with our previous observation using vit and mt-vit ERE sequences (*12*). The difference in the degree of sequence specificity highlights intrinsic differences in DNA binding properties between receptor subtypes, despite the high degree of conservation (96% identical) in their DNA-binding domains (*28*).

Competition Assay for Screening the Affinity of the ER for Various ERE Sequences Based on One Surface Preparation. To compare the subtle differences in the ability of receptors to bind to various ERE sequences with the direct assay approach, DNA molecules must be immobilized with identical surface density. For screening a large quantity of

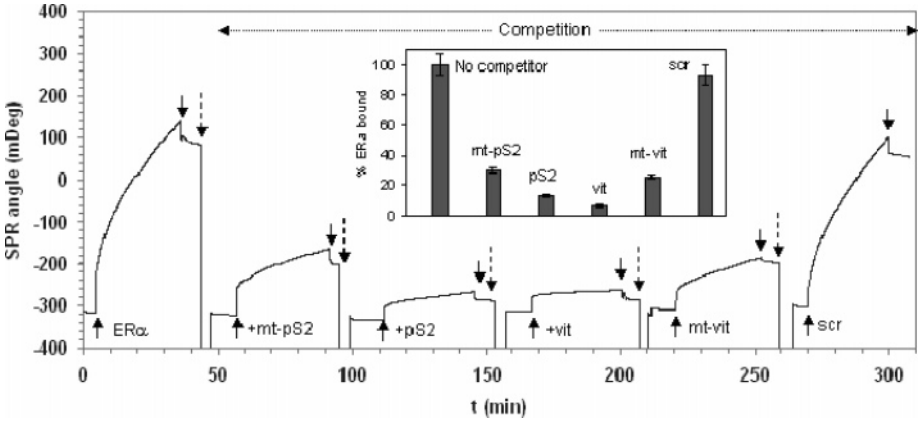

FIGURE 3: Competition assay performed for ERα on a pS2 ERE-immobilized surface (DNA immobilization not shown). The binding of ERα (110 nM) in the absence of competitors is followed by a sequential binding of ERα (110 nM) in the presence of a 3-fold excess of competitors, i.e., mt-pS2, pS2, vit, mt-vit, or scr ERE. The down arrows indicate the time when the receptor solutions are replaced with HEPES buffer. The dashed arrows indicate the time when 0.1% SDS is applied to dissociate the bound protein. The binding in the absence of competitor DNA is set as 100% and compared with the bindings in the presence of competitors (see the inset). The curve is a differential curve from the sample channel and a reference channel where the surface was left untreated with ERE.

sequences, immobilization of individual DNA is time-consuming and DNA density must be identical across the sequences that are being studied. We thus adopted a competition assay approach (Scheme 1B) to assess the relative affinity of ER for various ERE sequences with one surface preparation instead of individual DNA immobilization.

Figure 3 shows the sensorgram of a competition assay performed for ERα on a pS2 ERE (500 nM) immobilized surface. The ERα binding in the absence of competitor DNA is followed by bindings of ERα in the presence of a 3-fold excess of competitors, i.e., non-biotinylated mt-pS2, pS2, vit, mt-vit, and scr EREs. In this experiment, the second channel was left unmodified with DNA to correct for refractive index changes upon receptor binding. The reference signal is then subtracted from that in the sample channel to give the differential curve shown in Figure 3. Depending on the affinity of ERα for different competitors, the reactivity of ERα is inhibited to different extents, which is evidenced by the reduced level of binding to the immobilized pS2. Among the tested competitor sequences, vit ERE leads to the most pronounced reduction, indicating that this sequence has the strongest affinity for ERα compared to the others. Smaller reductions are observed when the competitors differ from the vit ERE by one (pS2) or more base pairs (mt-vit, mt-pS2, and non-ERE). According to the percentage of the ERα binding amount in the presence of competitors (see the inset of Figure 3), we find the following ERα affinity order: vit > pS2 > mt-vit ≥ mt-pS2 > scr ERE (GREB1 is not tested). This order is in agreement with the sequence-dependent binding amount determined using the direct assay approach. With this competition assay approach, a large number of DNA sequences can be assessed with one surface preparation.

In a similar fashion but via immobilization of A2 ERE, the inhibitions of ERα by 1-, 3-, 5-, 8-, 10-, and 20-fold excesses of competitors were performed. The level of bound receptors in the absence of competitor DNA was set at 100%. The competition at a certain concentration was calculated with the relation percentage of binding value (% binding) = [(signal obtained at a certain concentration of competitor)/(signal obtained without competitor)] × 100. The plots of the percent binding of ERα to immobilized vit ERE versus

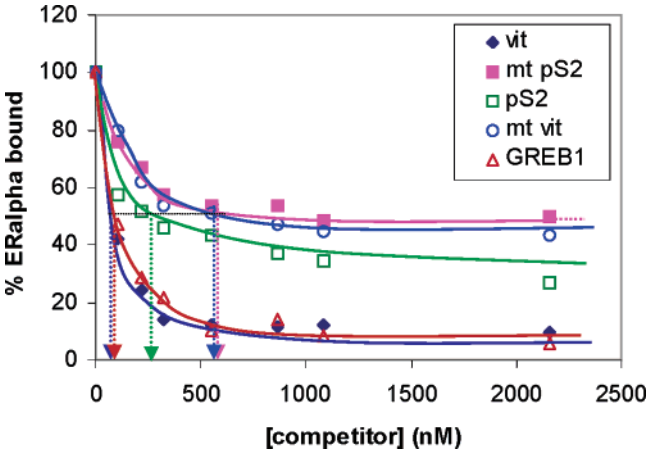

FIGURE 4: Competition profile of the binding of ERα to a vit ERE-immobilized surface in the presence of different competitors at 1-, 3-, 5-, 8-, 10-, and 20-fold excesses of the receptor. The receptor binding signal in the absence of competitors is set as 100% and compared with the signals in the presence of competitors. The concentration of the competitors at which the level of ERα−vit ERE binding is reduced by 50% (IC_{50}) is estimated to be 60, 70, 255, 580, and 600 nM for the vit, GREB1, pS2, mt-vit, and mt-pS2 sequences, respectively.

competitor concentrations yield the competition profiles (Figure 4), from which the concentrations of competitors required to decrease the level of ERα-vit−ERE binding by 50% (IC_{50}) were estimated. This value is indicative of the relative affinity of the protein for the competitor DNA (*29*). We observed again a clear trend of decreasing affinity (increasing IC_{50}): vit ≅ GREB1 > pS2 > mt-vit ≥ mt-pS2.

In comparison to the direct assay, this competition assay approach eliminates the need to immobilize individual ERE sequences. This not only saves time but also removes systematic errors that may be introduced by inconsistent surface preparations.

Dissociation Assay for the Determination of ER−ERE Binding Stoichiometry. Protein−DNA binding stoichiometry is an important parameter related to binding mechanisms. To determine the binding stoichiometry, one can titrate a known amount of immobilized DNA with increasing receptor concentrations to find the amount of receptor that saturates the DNA (*9*, *10*, *12*). However, this method would consume

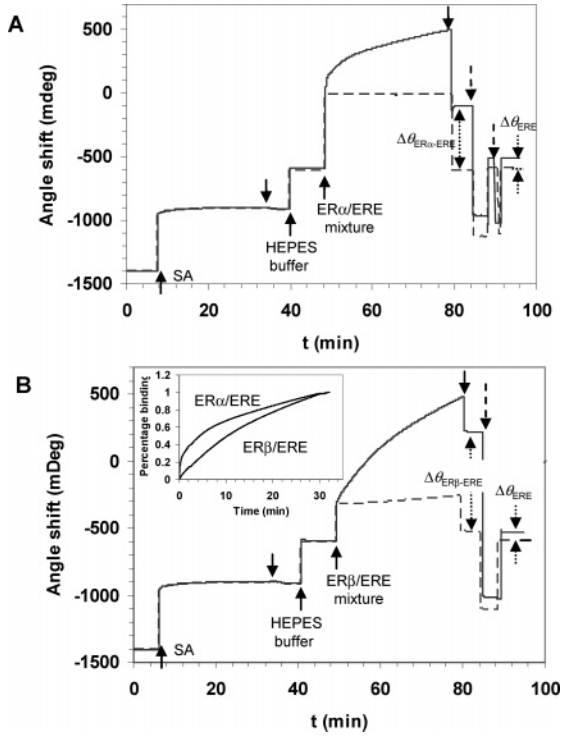

FIGURE 5: Determination of (A) ERα− and (B) ERβ−vit ERE binding stoichiometry using the dissociation assay. The SA-immobilized surface is reset using HEPES buffer containing 200 mM KCl. The preincubated biotinylated ER/ERE mixture (50 and 500 nM, respectively) in HEPES buffer is then passed through to allow the ER−ERE complexes to bind to the surface through the biotin residues on the ERE. At ~30 min, the binding was stopped by rinsing the liquid cell using HEPES buffer (down arrows). SDS (0.1%) is then applied (dashed arrows) to dissociate the bound protein, followed by resetting the surface in HEPES buffer. The SDS treatment can be repeated [for ERα (A) for example] to confirm the complete removal of the bound receptor. Control experiments (dashed lines) were conducted with a non-biotniylated ERE/ER mixture to check the nonspecific adsorption to the streptavidin surface. The inset in panel B shows the normalized complex binding (%) after correction of the bulk buffer effect.

a great amount of protein and is time-consuming. Moreover, saturation of surface-immobilized DNA may not be fully achievable due to the diffusion limitation. Inspired by the possibilities that the SA-treated surface can capture biotinylated molecules and a small amount of SDS can dissociate bound ER, we developed an alternative assay approach, denoted as the dissociation assay (Scheme 1C), for the easy determination of ER−ERE binding order.

Panels A and B of Figure 5 are the sensorgrams of the dissociation assay performed for ERα and ER*β*, respectively. In these experiments, 50 nM biotinylated vit ERE was incubated with 500 nM ERα or ER*β* in HEPES buffer containing 200 mM KCl (the use of excess amounts of the receptor ensures the biotinylated ERE is saturated during the formation of the ER−ERE complex). When exposed to a SA surface, the ER−ERE complexes are anchored through the biotin residue on the DNA. At the end of the complex assembly, 0.1% SDS dissociates the bound receptors. When the samples are rinsed with buffer solution, the receptors are removed, leaving the biotinylated ERE anchored on the surface. In the reference channel, non-biotinylated ERE preincubated with receptors under the same conditions is applied to check for nonspecific adsorptions. Similar experiments were conducted for receptor−ERE incubation at a lower salt concentration of 100 mM KCl. Table 2 summarizes the SPR angle shifts caused by the specific assembly of ER−ERE complexes and the remaining biotinylated ERE after removal of the receptors, from which the ER/ERE binding ratio (stoichiometry) is calculated.

Results in Table 2 confirm that ERα binds to ERE as a dimer (*10*, *30*) at 200 mM KCl, but probably as a tetramer under the lower-salt condition, and ER*β* is found to bind to ERE at higher levels (ER*β*/ERE ratio of 4−6) than ERα. A similar salt concentration dependence of ER−ERE binding stoichiometry has been reported by Royer and co-workers using a fluorescence anisotropy method (*30*, *31*). They estimated the relative binding stoichiometry under lower and higher salt conditions by determining the size of the ER−ERE complexes. Using SPR quantification of the amount of protein and DNA binding, we are able to quantify the binding order with a higher degree of certainty.

One of the advantages of SPR analysis over traditional end-point assays is its real-time measurement of the binding process. The inset in Figure 5B is the normalized SPR angle shifts for the assembly of biotinylated ERα− and ER*β*−ERE complexes after correction of the buffer jump. It is obvious that the ER*β* complex binds to the surface more slowly than ERα complex. The question of how these distinct binding kinetics may be determined by the physical properties of the complexes, e.g., hydrodynamic size (four ER*β* or two ERα molecules per ERE; see Table 2) and overall surface charge, etc., that maybe affect the diffusion of the complexes from solution to surface would have to subjected to further investigation.

Table 2: Determination of ER−vit ERE Binding Stoichiometry Using the Dissociation Assay Approach[a]

step	100 mM KCl	200 mM KCl	step	100 mM KCl	200 mM KCl
ERα−ERE			ER*β*−ERE		
millidegrees	655	525	millidegrees	952	748
ERE			ERE		
millidegrees	53	75	millidegrees	61	70
picomoles per square centimeter[b]	2.0	2.9	picomoles per square centimeter[b]	2.4	2.7
ERα			ER*β*		
millidegrees	602	450	millidegrees	892	687
picomoles per square centimeter[b]	7.6	5.7	picomoles per square centimeter[b]	13.9	10.6
ERα−ERE	3.7	1.9	ER*β*−ERE	5.9	3.9
moles per mole			moles per mole		

[a] SPR angle shifts (average values from triplicate repeat experiments; variation within 5%) caused by the assembly of ER−ERE complexes and remaining ERE are used to calculate the binding capacity and binding stoichiometry. [b] Receptor and DNA binding capacity in picomoles per square centimeter is calculated using a SPR mass sensitivity of 120 mdeg = 100 ng/cm^2, and the molecular masses of 21.4, 66.5, and 53.4 kDa for A2 ERE, ERα, and ER*β*, respectively.

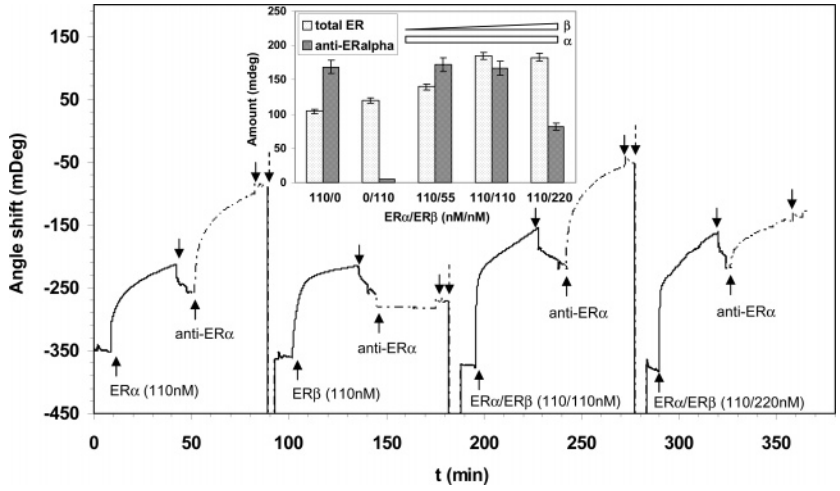

FIGURE 6: Sandwich assay for detection of specific ER subtype and the association of ERα and -β with ERE. The sensorgram shows the binding of ERα (110 nM), ERβ (110 nM), and ERα/ERβ mixtures at input ratios of 1:1 (110 and 110 nM, respectively) and 1:2 (110 and 220 nM, respectively) to immobilized vit ERE (24 mdeg), and each is followed by the binding of anti-ERα (10 μg/mL). The curve is a differential curve from the sample channel and a reference channel where the surface was left untreated with ERE. The down arrows indicate the time when the receptor and antibody solutions are replaced (surface is rinsed) with HEPES buffer. The dashed arrows indicate the time when 0.1% SDS is applied to regenerate the immobilized DNA. The inset summarizes the amounts of total ER bound at different α:β input ratios and the subsequent anti-ERα amount.

Sandwich Assay for Detecting Possible Competition and Association of ERα and ERβ on ERE. In gel shift assays, antibodies specific to a particular receptor subtype are used to identify the receptor−DNA complex, by supershifting the retarded complex bands (*17*, *19*, *20*). In this study, we adopt a similar concept and develop a sandwich assay (Scheme 1D) to identify the protein bound to immobilized DNA. Following the binding of a receptor mixture, an anti-ERα antibody is applied to identify and sandwich its specific antigen (ERα). With this assay scheme, we can quantitate the amount of a specific receptor bound from a mixture of different receptors. We can also verify how ERα and ERβ may compete or associate to form heterodimers when bound to ERE (*32*, *33*).

Figure 6 shows the binding of receptors (110 nM ERα or ERβ alone and ERα/ERβ mixtures at concentrations of 110 and 110 nM and 110 and 220nM, respectively) to immobilized vit ERE (from a 20 nM solution), and the binding of anti-ERα in a successive step, with the subtraction of reference signals from a reference channel that carries no ERE. The inset in Figure 6 summarizes the total receptor and antibody binding signals displayed in Figure 6 (including those from an α/β mixture of 110 and 55 nM, respectively, the binding curve of which is not shown). Results of the first two cycles show that when ERβ alone binds to ERE, no significant antibody signal is detected because of the high specificity of this antibody toward ERα whereas when ERα alone binds, the anti-ERα binding is readily detectable.

Before we discuss the implication of the receptor and antibody signals in Figure 6, we show in Figure 7 results from a separate experiment in which ERα alone binds to immobilized vit ERE at different DNA surface densities, followed by the binding of anti-ERα. The ERα binding amount is determined by the ERE surface density as expected. The successive anti-ERα signals are found to be linearly related to the ERα binding signals ($r^2 = 0.97$). This linear correlation indicates that the sandwich SPR approach using specific antibody binding can provide quantitative analysis of bindings of ER subtype.

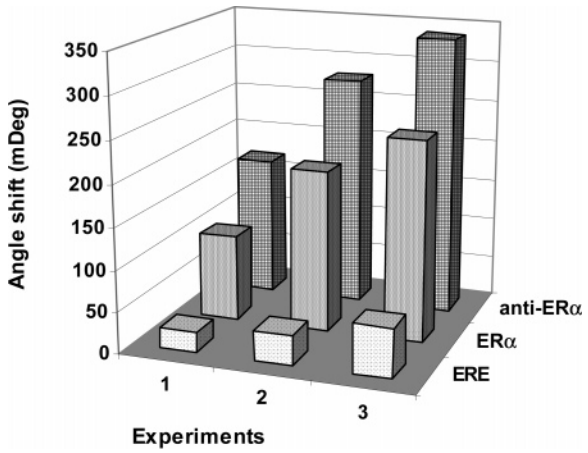

FIGURE 7: Binding signals for binding of ERα at a fixed receptor concentration (110 nM) to immobilized vit ERE with different surface coverages (26, 38, and 65 mdeg), obtained using a concentration of 20−50 nM. The ERα binding is found to be linearly related to the ERE amount. The subsequent anti-ERα (10 μg/mL) binding is also found to be linearly related to ERα binding.

In Figure 6, we show that when there are inputs of ERβ in 110 nM ERα, the total receptor binding signals increase steadily with the increase in ERβ concentration and saturation is reached when the total ER concentration is 220 nM (no further increase in the receptor binding signals at the total concentration of 330 nM), whereas the trend of antibody signals follows a different pattern. First, the inclusion of 55 and 110 nM ERβ has no significant effect on the amount of ERα bound to ERE, as evidenced by their antibody signals being similar to that in the case of ERα alone. Previous studies have shown that the α−α homodimer and the α−β heterodimer have significantly higher binding affinity for ERE than the β−β homodimer or the β−β−β−β tetramer (*32*, *33*); thus, in the presence of 55 nM ERβ (mixture of 110 and 55 nM), the ERα homodimer is likely to be predominant, with some α−β heterodimer. In other words, the binding of ERβ from this mixture is likely due to its association with ERα. As the ERβ input concentration

increases to 110 nM, the total acceptor binding amount is further increased. Using the linear relationship between anti-ERα and ERα signals, the similar antibody amount observed for ERα alone and for this mixture of 110 and 110 nM suggests that there are similar amounts of ERα (~100 mdeg) bound on the ERE. This in turn indicates that in the total amount of receptors bound (~185 mdeg) from this mixture, ERβ takes up ~85 mdeg. Thus, the molar ratio of bound ERα and ERβ is ~1:1, taking into the account the molecular masses of 66.5 and 53.4 kDa for the α and β subtypes, respectively. This result further validates the observation from the gel shift assay that in a mixture of equivalent α and β molar input, α−β heterodimer dominates the binding (*32*).

A reduction in the magnitude of the antibody signal, and thus the ERα amount, was observed when the ERβ concentration is twice that of ERα (α and β input of 110 and 220 nM, respectively). Using the linear relationship between anti-ERα and ERα signals, the amount of ERα present at the surface, from this input ratio of 1:2, could be approximately half that of other molar input ratios. The more significant ERβ binding at this input ratio could be attributed to the successive competition of the ERβ homodimer or tetramer with ERα, in addition to the formation of the α−β heterodimer.

In gel shift assays, antibodies specific to receptor subtypes are used for qualitative identification of the receptor−DNA complex (*10*, *21*, *32*). Whereas using an antibody in the SPR sandwich assay allows quantitation of the specific proteins, this assay can readily extend its usefulness in detection of specific receptor binding with DNA from raw nuclear extractions.

CONCLUSION

Using the estrogen receptors and their response elements as a model system, we have demonstrated the versatilities and advantages of the SPR assays which can alleviate many of the problems associated with traditional biological methods. First, DNA surface density control through immobilization allows for an accurate comparison of receptors' ability to bind to various sequences, whereas in gel shift assays, the intensity of the retarded protein−DNA bands for different sequences is not necessarily an accurate quantification of the amount of complex formed as it is dependent on the uniformity of DNA radiolabeling. Second, with the regeneration strategy in SPR analysis, the immobilized DNA can be reused and the binding behavior of various receptors and/or receptors under competition with a specific sequence can be compared in one experiment. Third, the quantification of molecular binding amount in SPR allows the determination of receptors' binding capacity and stoichiometry and a quantitative identification of the ER−DNA complex. Finally, the real-time information for ER−DNA complex assembly, for example, underlines their distinct physical properties.

By making use of the versatility described above, we have discovered distinct DNA binding behaviors of the two ER subtypes, which may further our understanding of how these receptors regulate gene expression differently. We believe that the assay schemes we developed for the ER−ERE interactions can steadily extend their usefulness in studying other protein−DNA and biomolecular binding interactions.

SUPPORTING INFORMATION AVAILABLE

Concentration-dependent ERE binding amount and ERE surface density. This material is available free of charge via the Internet at http://pubs.acs.org.

REFERENCES

1. Sladek, R., and Giguere, V. (1998) Initial characterization of new orphan receptor, in *Nuclear Receptors: A Practical Approach* (Picard, D., Ed.) pp 29−69, Oxford University Press, Oxford, U.K.
2. Gong, P., Lee, C. Y., Gamble, L. J., Castner, D. G., and Grainger, D. W. (2006) Hybridization behavior of mixed DNA/alkylthiol monolayers on gold: Characterization by surface plasmon resonance and ^{32}P radiometric assay, *Anal. Chem. 78*, 3326−3334.
3. Kanoh, N., Kyo, M., Inamori, K., Ando, A., Asami, A., Nakao, A., and Osada, H. (2006) SPR imaging of photo-cross-linked small-molecule arrays on gold, *Anal. Chem. 78*, 2226−2230.
4. Homola, J. (2003) Present and future of surface plasmon resonance biosensors, *Anal. Bioanal. Chem. 377*, 528−539.
5. Karlsson, R. (2004) SPR for molecular interaction analysis: A review of emerging application areas *J. Mol. Recognit. 17*, 151−161.
6. Schubert, F., Zettl, H., Hafner, W., Krauss, G., and Krausch, G. (2003) Comparative thermodynamic analysis of DNA−protein interactions using surface plasmon resonance and fluorescence correlation spectroscopy, *Biochemistry 42*, 10288−10294.
7. Shumaker-Parry, J. S., Zareie, M. H., Aebersold, R., and Campbell, C. T. (2004) Microspotting streptavidin and double-stranded DNA arrays on gold for high-throughput studies of protein−DNA interactions by surface plasmon resonance microscopy, *Anal. Chem. 76*, 918−929.
8. Maillart, E., Brengel-Pesce, K., Capela, D., Roget, A., Livache, T., Canva, M., Levy, Y., and Soussi, T. (2004) Versatile analysis of multiple macromolecular interactions by SPR imaging: Application to p53 and DNA interaction, *Oncogene 23*, 5543−5550.
9. Smith, E. A., Erickson, M. G., Ulijasz, A. T., Weisblum, B., and Corn, R. M. (2003) Surface plasmon resonance imaging of transcription factor proteins: Interactions of bacterial response regulators with DNA arrays on gold films, *Langmuir 19*, 1486−1492.
10. Cheskis, B. J., Karathanasis, S., and Lyttle, C. R. (1997) Estrogen receptor ligands modulate its interaction with DNA, *J. Biol. Chem. 272*, 11384−11391.
11. Chen, J. Q., Eshete, M., Alworth, W. L., and Yager, J. D. (2004) Binding of MCF-7 cell mitochondrial proteins and recombinant human estrogen receptors α and β to human mitochondrial DNA estrogen response elements, *J. Cell. Biochem. 93*, 358−373.
12. Su, X., Lin, C. Y., O'Shea, S. J., Teh, H. F., Peh, W. Y. X., and Thomsen, S. J. (2006) Combinatorial application of surface plasmon resonance spectroscopy and quartz crystal microbalance for studying nuclear hormone receptor−response element interactions, *Anal. Chem. 78*, 5552−5558.
13. Su, X., Robelek, R., Wu, Y. J., Wang, G. Y., and Knoll, W. (2004) Detection of point mutation and insertion mutations in DNA using a quartz crystal microbalance and MutS, a mismatch binding protein, *Anal. Chem. 76*, 489−494.
14. Wegner, G. J., Lee, H. J., Marriott, G., and Corn, R. M. (2003) Fabrication of histidine-tagged fusion protein arrays for surface plasmon resonance imaging studies of protein−protein and protein−DNA interactions, *Anal. Chem. 75*, 4740−4746.
15. Lin, L., Harris, J. W., Thompson, G. R., and Brody, J. P. (2004) Surface plasmon resonace-based sensors to identify cis-regulatory elements, *Anal. Chem. 76*, 6555−6559.
16. Loven, M. A., Wood, J. R., and Nardulli, A. M. (2001) Interactions of estrogen receptors α and β with estrogen response elements, *Mol. Cell. Endocrinol. 181*, 151−163.
17. Yi, P., Driscoll, M. D., Huang, J., Bhahat, S., Hilf, R., Bambara, R. A., and Muyan, M. (2002) The effects of estrogen-responsive element- and ligand-induced structural changes on the recruitment of cofactors and transcriptional responses by ERα and ERβ, *Mol. Endocrinol. 16*, 674−693.
18. Crowther, J. R. (1995) *ELISA Theory and Practice*, pp 35−50, Humana Press, Totowa, NJ.

19. Muramatsu, M., and Inoue, S. (2000) Estrogen Receptors: How Do They Control Reproductive and Nonreproductive Functions? *Biochem. Biophys. Res. Commun. 270*, 1−10.
20. Melamed, M., Arnold, S. F., Notidess, A. C., and Sasson, S. (1996) Kinetic analysis of the interaction of human estrogen receptor with an estrogen response element, *J. Steroid Biochem. Mol. Biol. 57*, 153−159.
21. Hyder, S. M., Chiappeta, C., and Stancel, G. M. (1999) Interaction of human estrogen receptors α and *β* with the same naturally occurring estrogen response elements, *Biochem. Pharmacol. 57*, 597−601.
22. Asano, K., Ono, A., Hashimoto, S., Inoue, T., and Kanno, J. (2004) Screening of endocrine disrupting chemicals using a surface plasmon resonance sensor, *Anal. Sci. 20*, 611−616.
23. Klein-Hitpass, L., Ryffel, G. U., Heitlinger, E., and Cato, A. B. C. (1998) A 13 bp palindrome is a functional estrogen responsive element and interacts specifically with estrogen receptor, *Nucleic Acids Res. 16*, 647−663.
24. Bourdeau, V., Deschênes, J., Métivier, R., Nagai, Y., Nguyen, D., Bretschneider, N., Gannon, F., White, J. H., and Mader, S. (2004) Genome-wide identification of high-affinity estrogen response elements in human and mouse, *Mol. Endocrinol. 18*, 1411−1427.
25. Nunez, A. M., Jakowlev, S., Briand, J. P., Garie, M., Krust, A., Rio, M. C., and Chambon, P. (1987) Characterization of the estrogen-induced pS2 protein secreted by the human breast cancer cell line MCF-7, *Endocrinology 121*, 1759−1765.
26. Su, X. D., Wu, Y. J., Robelek, R., and Knoll, W. (2005) Surface plasmon resonance spectroscopy and quartz crystal microbalance study of streptavidin film structure effects on biotinylated DNA assembly and target DNA hybridization, *Langmir 21*, 348−353.
27. Knoll, W., Zizlsperger, M., Liebermann, T., Arnold, S., Badia, A., Liley, M., Piscevic, D., Schmitt, F.-J., and Spinke, J. (2000) Streptavidin array as supramolecular architectures in surface plasmon optical sensor formats, *Colloids Surf., A 161*, 115−137.
28. Mosselman, S., Polman, J., and Dijkema, R. (1996) ER*β*: Identification and characterization of a novel human estrogen receptor, *FEBS Lett. 392*, 49−53.
29. Escande, A., Pillon, A., Servant, N., Cravedi, J., Larrea, F., Muhn, P., Nicolas, J., Cavaillès, V., and Balaguer, P. (2006) Evaluation of ligand selectivity using reporter cell lines stably expressing estrogen receptor α or *β*, *Biochem. Pharmacol. 71*, 1459−1469.
30. Boyer, M., Poujol, N., Margeat, E., and Royer, C. A. (2000) Quantitative characterization of the interaction between purified human estrogen receptor α and DNA using fluorescence anisotropy, *Nucleic Acids Res. 28*, 2494−2502.
31. Margeat, E., Bourdoncle, A., Maegueron, R., Poujol, N., Cavailles, V., and Royer, C. (2003) Ligands differentially modulate the protein interactions of the human estrogen receptors α and *β*, *J. Mol. Biol. 326*, 77−92.
32. Pettersson, K., Grandien, K., Kuiper, G. G. J. M., and Gustafsson, J. (1997) Mouse estrogen receptor *β* forms estrogen response element binding heterodimers with estrogen receptor α, *Mol. Endocrinol. 11*, 1486−1496.
33. Cowley, S. M., Hoare, S., Mosselman, S., and Parker, M. G. (1997) Estrogen receptors α and *β* form heterodimers on DNA, *J. Biol. Chem. 272*, 19858−19862.

BI061903T